Heliyon 10 (2024) e31860

Contents lists available at ScienceDirect

Heliyon

journal homepage: www.cell.com/heliyon

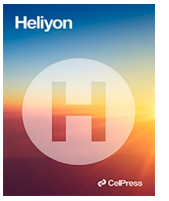

Research article

Qi Lang formula relieves constipation via targeting SCF/c-kit signaling pathway: An integrated study of network pharmacology and experimental validation

Jiacheng Li [a,b], Yugang Fu [a,b], Yanping Wang [a,b], Yiyuan Zheng [a], Kehui Zhang [a], Yong Li [a,*]

[a] Shanghai Municipal Hospital of Traditional Chinese Medicine, Shanghai University of Traditional Chinese Medicine, Shanghai, 200071, China
[b] Shanghai University of Traditional Chinese Medicine, Shanghai, 200071, China

ARTICLE INFO

Keywords:
Qi Lang formula
UPLC-MS/MS
Constipation
Network pharmacology
SCF/c-Kit

ABSTRACT

Background: Constipation is one of the chronic gastrointestinal functional diseases that affects the quality of life. While Qi Lang Formula (QLF) has demonstrated effectiveness in alleviating constipation symptoms, its precise mechanism remains elusive.
Methods: QLF was analyzed using UPLC-MS/MS. Targets for QLF were collected from SwissADME, Herb, ITCM databases, and constipation-related targets from scRNA-seq and Genecards databases. Overlapping targets suggested potential QLF therapy targets for constipation. Enrichment analysis used the KOBAS database. A "drug-ingredient-target" network was constructed with Cytoscape, and AutoDock verified active ingredient binding. H&E staining assessed colonic mucosa changes, TEM examined ICC structural changes. ELISA measured neurotransmitter levels, and Western blot verified QLF's effect on target proteins. ICC proliferation was observed through immunofluorescence.
Results: We identified 89 targets of QLF associated with ICC-related constipation, with c-Kit emerging as the pivotal target. Molecular docking studies revealed that Atractylenolide III, Apigenin, Formononetin, Isorhamnetin, Naringenin, and Ononin exhibited strong binding affinities for the c-Kit structural domain. QLF significantly enhanced first stool passage time, fecal frequency, fecal moisture content, and intestinal propulsion rate. Further analysis unveiled that QLF not only restored neurotransmitter levels but also mitigated colon muscular fiber ruptures. ICC ultrastructure exhibited partial recovery, while Western blot confirmed upregulated c-Kit expression and downstream targets. Immunofluorescence results indicated ICC proliferation post QLF treatment in rat colon.
Conclusion: Our findings suggest that QLF may promote ICC proliferation by targeting SCF/c-Kit and its downstream signaling pathway, thereby regulating intestinal motility.

1. Introduction

Constipation is a gastrointestinal functional disorder characterized by infrequent bowel movements, prolonged defecation time,

* Corresponding author. Department of Gastroenterology, Shanghai Municipal Hospital of Traditional Chinese Medicine, Shanghai University of Traditional Chinese Medicine, 274 Middle Zhijiang Road, Shanghai, 200071, China.
E-mail addresses: liyong_sci@126.com, liyong@shutcm.edu.cn (Y. Li).

https://doi.org/10.1016/j.heliyon.2024.e31860
Received 10 March 2024; Received in revised form 21 May 2024; Accepted 22 May 2024
Available online 23 May 2024

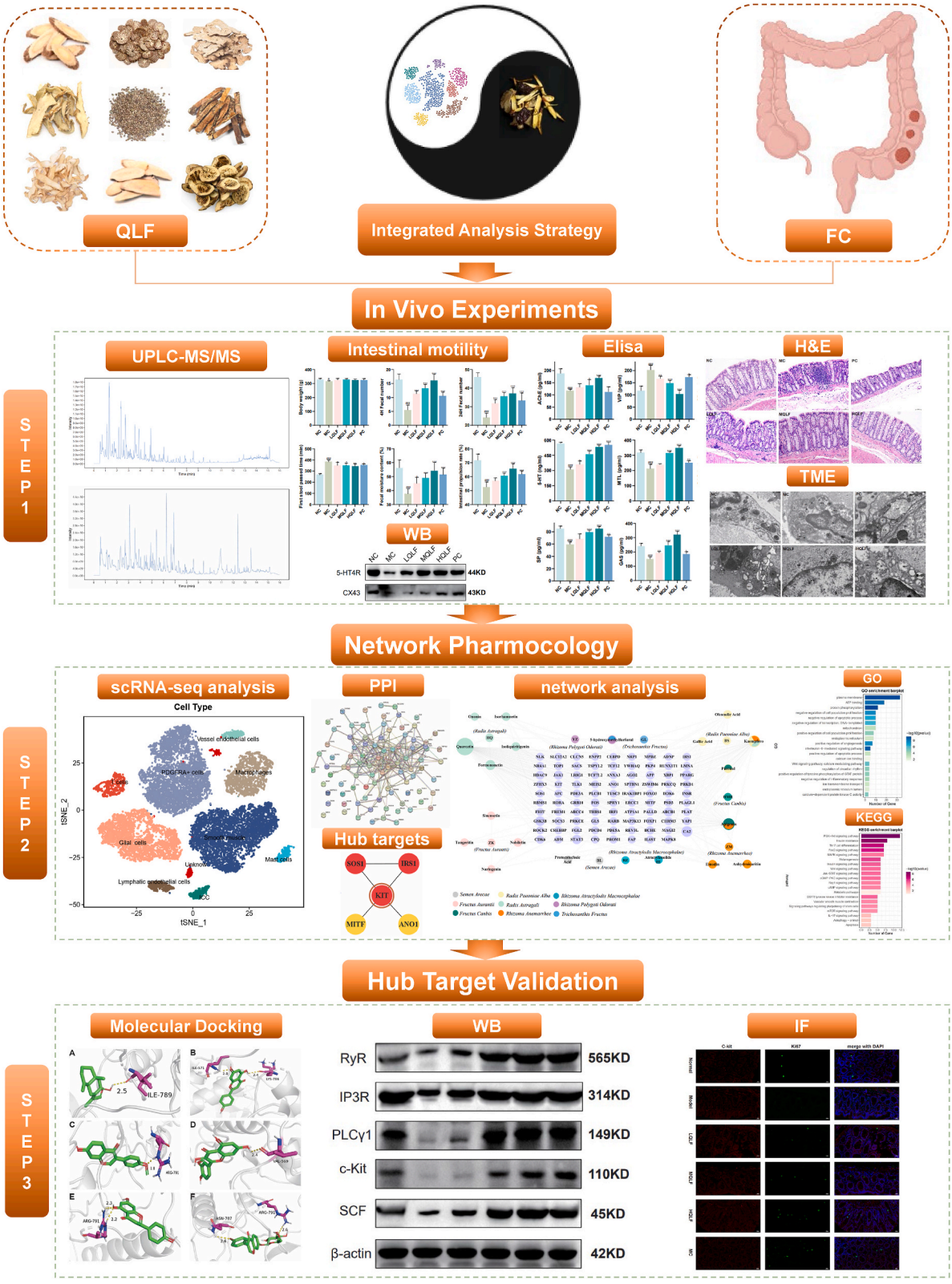

Fig. 1. Comprehensive workflow of the study.

difficulty passing stool, dry and hard stool, abdominal pain, and other symptoms. According to Rome IV, the global average prevalence of constipation is 10.1% [1]. In Europe and America, the incidence of constipation is as high as 14%–30%, whereas in China, the prevalence is approximately 8.5% [2–6]. Presently, primary constipation management strategies encompass dietary and lifestyle adjustments, rehabilitation training, surgical interventions, laxative administration, and medications to enhance bowel motility. However, their effectiveness is constrained, frequently failing to provide a lasting solution and potentially fostering a reliance on laxatives. These approaches often fall short of desired outcomes and may result in medication dependence for individuals with constipation. Past studies suggested that traditional Chinese medicine offered potential benefits with fewer side effects [7–10]. The Qilang formula (QLF) is proved to be effective for chronic constipation in clinical practice. Researchers observed increased levels of serum motilin (MTL), 5-hydroxytryptamine (5-HT), and short-chain fatty acids in feces, along with decreased serum NF-κB, TNF-α, IL-6, IL-12, and vasoactive intestinal peptide (VIP) after QLF treatment for constipation. This suggests that QLF may work by modulating these factors, but its precise pharmacological mechanism remains uncertain.

Interstitial cells of Cajal (ICC) were pacemaker cells mainly located in the muscular layer of the gastrointestinal tract [11–13]. The number and structure of ICC were associated with gastrointestinal motility [14,15]. Studies showed that KIT (also known as KIT proto-oncogene, c-Kit, and CD117), a cell surface receptor tyrosine kinase, was a marker of ICC in the digestive tract [16]. The SCF/c-Kit signaling pathway could affect the differentiation, proliferation, and phenotype maintenance of ICC. Furthermore, it was essential for the generation of slow-wave activity in the gastrointestinal muscles [17,18]. Studies indicated that constipated patients had fewer or less dense ICC in the colon than normal individuals, and cell morphology changes, such as the shortening of synapses, and the alteration or ablation of the colonic ICC network, could lead to colonic motility dysfunction, such as constipation [19]. Another study found that the epidural infusion of morphine combined with low-dose naloxone could effectively inhibit rabbit gastrointestinal motility by reducing ICC in the proximal colon of rabbits [20]. In summary, ICC was closely related to the occurrence of constipation. Therefore, this study explored the effect of QLF on ICC to investigate the mechanism of QLF in treating constipation.

In our research, we employed scRNA-seq data combined with the Genecards database to identify targets related to ICC-associated constipation. We then compared drug and disease targets to identify those QLF addresses when countering ICC-associated constipation. Through Western blot (WB) experiments, we observed that QLF up-regulated the protein expression of SCF/c-Kit signaling pathway. Immunofluorescence (IF) experiments indicated that QLF promoted ICC proliferation. In summary, QLF may alleviate constipation symptoms by promoting ICC proliferation, restoring intestinal motility, and upregulating the SCF/c-Kit signaling pathway and their downstream targets. The workflow of this study is shown in Fig. 1.

2. Materials and methods

2.1. Materials

The Qilang formula is provided by Shanghai Wanshicheng Pharmaceutical Co., Ltd. (Shanghai, China). Mosapride citrate was purchased from Chengdu Kanghong Pharmaceutical Co., Ltd. (Chengdu, China). Diphenoxylate was purchased from Shandong Renhetang Pharmaceutical Co., Ltd. (Linyi, China). Motile (MTL), gastrin (GAS), substance P (SP), 5-hydroxytryptamine (5-HT), acetylcholinesterase (AChE) and vasoactive intestinal peptide (VIP) ELISA kits were purchased from Shanghai Primacy Biotechnology Co., Ltd. (Shanghai, China). Powdered activated carbon and gum Arabic from Shanghai McLean Biochemical Technology Co., Ltd. (Shanghai, China).

2.2. Preparation and qualitative analysis of QLF

QLF consists of 9 traditional chinese herbs, including *Radix Astragali, Semen Arecae, Fructus Aurantii, Rhizoma Anemarrhee, Rhizoma Polygonati Odorati, Trichosanthis Fructus, Rhizoma Atractylodis Macrocephalae, Fructus Canbis*, and *Radix Paeoniae Alba*. The ratio of each component is as the following 15:15:15:9:15:15:30:30:30. The QLF used in our experiment is provided by Shanghai Wanshicheng Pharmaceutical Co., Ltd.

UPLC-MS/MS analysis was performed on an UHPLC system (Vanquish, Thermo Fisher Scientific) with a Waters UPLC BEH C18 column (100 mm*2.1 mm, 1.7 μm). The mobile phase is 0.1% formic acid aqueous solution (A) and 0.1% formic acid acetonitrile solution (B). Gradient elution procedure: 0–11 min, 85-25% A; 11–12 min, 25-2% A; 12–14min, 2-2% A; 14–14.1 min, 2–85% A. The column temperature was 50 °C, the flow rate was 0.5 mL· min-1, and the sample volume was 5 μL. An Orbitrap Exploris 120 mass spectrometer coupled with an Xcalibur software was employed to obtain the MS and MS/MS data based on the IDA acquisition mode. During each acquisition cycle, the mass range was from 100 to 1500, and the top four of every cycle were screened and the corresponding MS/MS data were further acquired. Sheath gas flow rate: 35 Arb, Aux gas flow rate: 15 Arb, Ion Transfer Tube Temp: 350 °C, Vaporizer Temp: 350 °C, Full MS resolution: 60000, MS/MS resolution: 15000, Collision energy: 16/38/42 in NCE mode, Spray Voltage: 5.5 kV (positive) or −4 kV (negative).

2.3. Animals

48 healthy male Wistar rats (12 weeks old) were provided by Sipeifu (Beijing) Biotechnology Co., Ltd. (certificate numbers: SCXK (Jing) 2019-0010; Beijing, China). The animal experimental procedures were approved by the Ethics Committee of Shanghai Traditional Chinese Medicine Hospital (Approved on February 9, 2022; NO.202201). All rats were kept in an animal laboratory with a specific pathogen free (SPF) environment (certificate numbers: SCXK (Hu) 2020-0014; Shanghai, China). Feeding conditions: Room

temperature maintained at (22 ± 4) °C, humidity at (52 ± 8) %, 12 h of daylight exposure per day, 12 h of darkness, free access to food and water.

2.4. Establishment of rat model and drug administration

After a 7-day adaptation period, 48 rats were randomly and evenly divided into the following 6 groups: Normal control group (Normal) received ultrapure water; Model group (Model) received diphenoxylate; Low-dose QLF group (LQLF) was induced with diphenoxylate and orally administered QLF at a dosage of 8.95 g/kg per day; Medium-dose QLF group (MQLF) was induced with diphenoxylate and orally administered QLF at a dosage of 17.89 g/kg per day; High-dose QLF group (HQLF) was induced with diphenoxylate and orally administered QLF at a dosage of 35.78 g/kg per day; Mosapride Citrate group (MC) received diphenoxylate and orally administered mosapride citrate at a dosage of 1.54 mg/kg per day. The MQLF dosage used in rats was calculated from clinical dosage using the following formula: MQLF dosage = 174 g × 6.17/60 kg. The clinical drug dosage of QLF was 174 g/person/day, and the average body weight of normal adults was 60 kg, resulting in an equivalent dose ratio of 6.17 between rats and humans. Except for the Normal group, all other groups were orally administered diphenoxylate at a dosage of 50 mg/kg/day for 14 consecutive days to establish the constipation rat model. All animals were orally administered ultrapure water, QLF or mosapride citrate tablets according to the designated dosages for a duration of 14 days.

2.5. Measurement of laxative effect of QLF on model rats

2.5.1. Calculation of first defecation time and fecal moisture content

The rats were fasted for 24 h prior to the final administration. Thirty minutes after the final administration, they were orally administered 1 ml of a 10% activated charcoal suspension. Normal drinking water and food intake were restored, and the rats were individually housed. The time of the first defecation was recorded. Rat feces were collected within a 4-h period and weighed fresh and dried. The feces were placed in a 90 °C electric constant temperature oven and continuously heated until a constant weight was obtained. Fecal moisture content was measured using the following formula: Fecal moisture content (%) = (wet weight - dry weight)/wet weight × 100%.

2.5.2. Determination of intestinal propulsion rate

After a 24-h fasting period following the last administration, the rats were orally administered 1 mL of a 10% activated charcoal suspension. Then, 30 min later, rats were anesthetized with an intraperitoneal injection of 50 mg/kg of pentobarbital sodium. and killed by bloodletting via the main abdominal vein. The entire length of the small intestine from the pylorus to the cecum was carefully removed. In a tension-free state, the total length of the small intestine (L1) and the distance from the pylorus to the leading edge of the black charcoal were measured (L2). The intestinal propulsion rate was calculated using the following formula: Intestinal propulsion rate = L2/L1 × 100%.

2.6. ELISA assay

Whole blood was collected while the serum was isolated through centrifugation. The level of MTL, GAS, SP, 5-HT, AChE and VIP were assayed by ELISA kits according to their protocols.

2.7. H&E staining

Fresh colon tissue was fixed in 10% buffered formali for at least 24 h, dehydrated, and then embedded in paraffin wax. Subsequently, 5-μm sections were cut and mounted on glass slides. One section per sample was subjected to hematoxylin-eosin (H&E) staining to evaluate histopathological changes.

2.8. Transmission electron microscopy (TEM)

We obtained about 1 mm^3 of proximal colon tissue, fixed it with 2.5% glutaraldehyde for 24h, then with 1% osmic acid for 2h, dehydrated it with ethanol and acetone gradient, embedded EMBed 812, and cut it into 60 nm ultra-thin sections on an ultra-micro microtome. 2% uranium acetate saturated alcohol solution and 2.6% lead citrate solution were stained for 8 min, avoiding carbon dioxide. We observed mitochondria, autophagosome and Rough endoplasmic reticulum of colonic ICC under a HITACHI HT7800 transmission electron microscope.

2.9. Western blot

Proteins from colon tissue were extracted with RIPA cracking buffers containing protease and phosphatase inhibitors (Beyotime, Shanghai, China, Cat# P0013C). After centrifugation at 12000 rpm for 10 min at 4 °C, the resulting supernatant was collected. Protein concentration was quantified using a BCA assay kit. Equal protein amounts were separated on SDS-PAGE gel, transferred onto a 0.45 μm PVDF membrane, and blocked with 5% BSA in TBST for 2 h at room temperature. Membranes were incubated overnight at 4 °C with primary antibodies, including anti-CX43 (Cat#AB11370; Abcam, UK), anti-RyR (Cat#AB2868; Abcam, UK), anti-PLCγ1

(Cat#AB76155; Abcam, UK), anti-IP3R (Cat#AB108517; Abcam, UK), anti-5-HT4R (Cat#DF3503; Affinity Biosciences, China), anti-*c*-Kit (Cat#18696-1-AP; Proteintech, China) and anti-SCF (Cat#26582-1-AP; Proteintech, China), followed by horseradish peroxidase-conjugated secondary antibodies. Enhanced chemiluminescence was used for band visualization, and Image J for band analysis and quantification.

2.10. Immunofluorescence staining

Paraffin was removed from the slide and fixed in 4% paraformaldehyde (PFA) at 4 °C for 10 min. The slides were washed three times with PBS and treated with 0.1% Triton X-100 at room temperature for 20 min.The slides were blocked with 3%BSA solution at room temperature for 30min. Subsequently, slides were incubated overnight at 4 °C with rabbit anti-rat Ki67 (Cat#AB16667; Abcam, UK) or rabbit anti-rat (Cat#18696-1-AP; Proteintech, China). After washing with PBS for three times, the slides were incubated with specific secondary antibody Alexa Fluor 488-conjugated Goat anti-Rabbit (Cat#GB25303; Servicebio, China) or Cy3 conjugated goat anti-rabbit (Cat#GB21303; Servicebio, China) at room temperature for 50 min away from light. Glass slides were prepared by mounting coverslips, and the DNA was counterstained using staining reagent containing DAPI (Servicebio). Image were obtained on NIKON ECLIPSE C1 fluorescence microscope (Nikon).

2.11. Network pharmacology

2.11.1. Drug targets of QLF

The results of UPLC-MS/MS combined with online databases such as PubMed (https://pubmed.ncbi.nlm.nih.gov/), Pubchem (https://pubchem.ncbi.nlm.nih.gov/), Herb (http://herb.ac.cn/), ITCM (http://itcm.biotcm.net/) and SwissADME (http://www.swissadme.ch/) were used to collect the active ingredients and related targets of QLF. The screening criteria for this study focused on two main parameters: Lipinski rule as "YES" and high gastrointestinal (GI) permeability. Following active ingredient screening with these criteria, drug targets were identified using Herb and ITCM databases, and relevant literature was consulted. To improve prediction accuracy, we consolidated data from these databases and removed duplicate entries.

2.11.2. Dimensionality reduction, clustering and annotation of scRNA-Seq data

Download 10 × scRNA-seq data from 14 colon samples from the GSE156905 series [21]. The "Seurat" R package was utilized to convert the data into a Seurat object. The following functions are all derived from Seurat. Quality control was conducted on the raw counts by calculating the percentages of mitochondrial and erythrocyte genes and excluding cells with low quality. Subsequently, homogenization was carried out using the "NormalizeData" function. The top 3000 highly variable features were filtered using the "FindVariableFeatures" function, and normalization was performed using the "ScaleData" function. Principal component analysis (PCA), a preliminary linear dimensionality reduction method, was applied to the scaled data, with batch effects eliminated using the default settings of Harmony (v1.0). The t-SNE algorithm, a nonlinear dimensionality reduction technique, was employed for cluster identification. Biologically significant cell types were annotated using the "FindAllMarkers" function to identify representative genes for each cluster in conjunction with typical cell markers.

2.11.3. Therapeutic targets for constipation

Genecards (https://www.genecards.org/) is a comprehensive and integrated database that utilizes a comprehensive calculation of disease-gene relevance scores to discover disease-associated genes. The target of constipation was collected with the keyword "constipation". ICC marker genes were obtained from the above scRNA-seq data. Conclusively, online Venn diagram tool “jvenn” (https://www.bioinformatics.com.cn/static/others/jvenn/example.html) was used to identify potential targets for QLF targeting ICC for constipation treatment.

2.11.4. Network construction

The potential targets of QLF targeting ICC against constipation were uploaded to the online tool String database (https://string-db.org/, Version: 12.0), and the minimum required interaction score was set to the highest confidence (0.4) as the threshold for screening. Subsequently, PPI and drug-ingredient-target networks were constructed using Cytoscape 3.9.1 software. The PPI network were further analyzed using the cytoHubba plugin to identify and prioritize the hub targets.

2.11.5. Enrichment analysis

The KOBAS database (http://kobas.cbi.pku.edu.cn/) was utilized for conducting GO and KEGG pathway enrichment analysis. The analysis results were filtered to select items with smaller *p*-values. R language was used to visualize the results. The top 20 significant KEGG pathways ($p < 0.05$) and the top 20 GO enrichments ($p < 0.05$) were plotted separately using bar graphs.

2.12. Molecular docking

Hub targets and active ingredients earlier filtered by network pharmacology were docking with AutoDock Vina. The structural formulas of active ingredients were obtained from the PubChem database (https://pubchem.ncbi.nlm.nih.gov/). Chem3D software was utilized to generate 3D structures of these active ingredients. The 3D structures of the target proteins were downloaded from the PDB database (http://www.rcsb.org/). PyMOL software was employed for protein-related operations, including dehydration and

hydrogenation. Furthermore, AutoDockTools (v1.5.7) software was utilized to search for ligand-binding pockets. Subsequently, the Vina script was applied to calculate molecular binding energy and visualize the molecular docking results. Finally, the obtained results were imported into PyMOL for visualization.

2.13. Statistical analysis

All data were presented as mean ± SD and analyzed using GraphPad Prism 9.0 for statistical analysis and data visualization. For comparisons between two groups, the Student's t-test was utilized. For comparisons involving more than two groups, one-way analysis of variance (one-way ANOVA) was performed. The p-value <0.05 was considered statistically significant for all results.

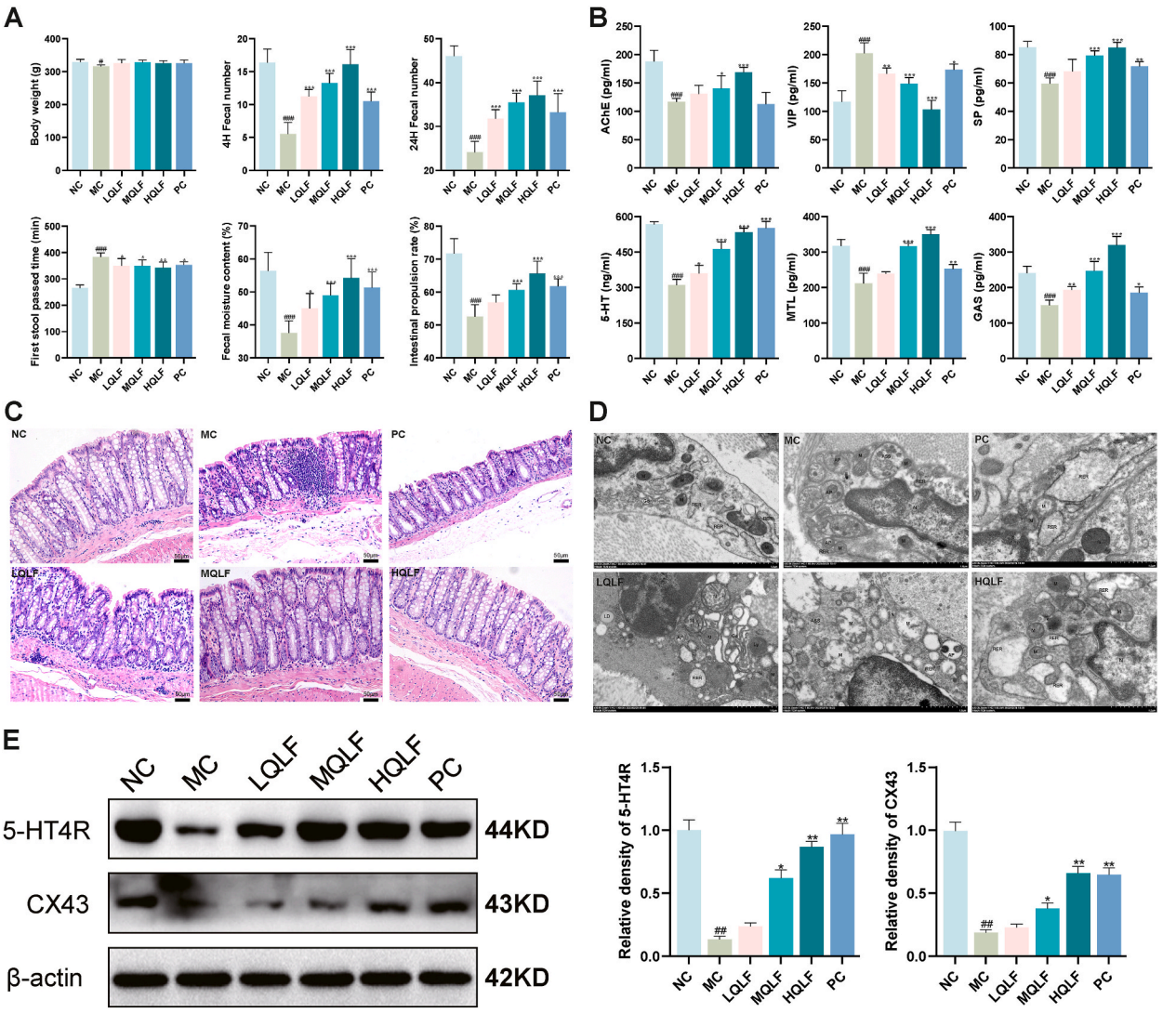

Fig. 2. QLF were effective in treating constipation. (A) Final body weight, fecal number, first defecation time, fecal moisture content and Intestinal propulsion rate were determined at the end of the study. (B) AChE, VIP, SP, 5-HT, MTL and GAS in serum were assayed by ELISA, n = 6. (C) Colon stained with H&E (original magnification, × 200). (D) Observation of mitochondria, autophagosome and rough endoplasmic reticulum of colonic ICC by transmission electron microscopy (original magnification, × 30.0k). (E) the protein levels of CX43 and 5-HT4R in colon tissue based on WB assay, n = 6. Data are expressed as mean ± SD. $^{\#}p < 0.05$, $^{\#\#}p < 0.01$, $^{\#\#\#}p < 0.001$, compared to the NC group. $^{*}p < 0.05$, $^{**}p < 0.01$, $^{***}p < 0.001$, compared to the MC group. **Abbreviations:** NC: normal control group; MC: model control group; PC: positive control group; LQLF: low dose of QLF (8.95 g/kg/day); MQLF: Medium high dose of QLF (17.89 g/kg/day); HQLF: high dose of QLF (35.78 g/kg/day). M: Mitochondria; RER: Rough endoplasmic reticulum; CF: Collagen filament; ASS: Autopolysosome; AP: Autophagosome; Ly: Lysosome; Go: Golgiapparatus; LD: Lipid droplet.

3. Results

3.1. Chemical composition analysis of QLF

The active ingredients of QLF were identified by UPLC-MS/MS. The total ion chromatogram is shown in Supplementary Fig. S1. The identification of the 19 ingredients in the QLF was conducted tentatively using retention times (RTs), molecular weight, and MS/MS fragment ions as criteria. Among them, 12 ingredients belonged to flavonoids, 2 belonged to terpenoids, 3 belonged to phenols, 1 belonged to anthraquinones, and 1 belonged to others (Supplementary Table S1).

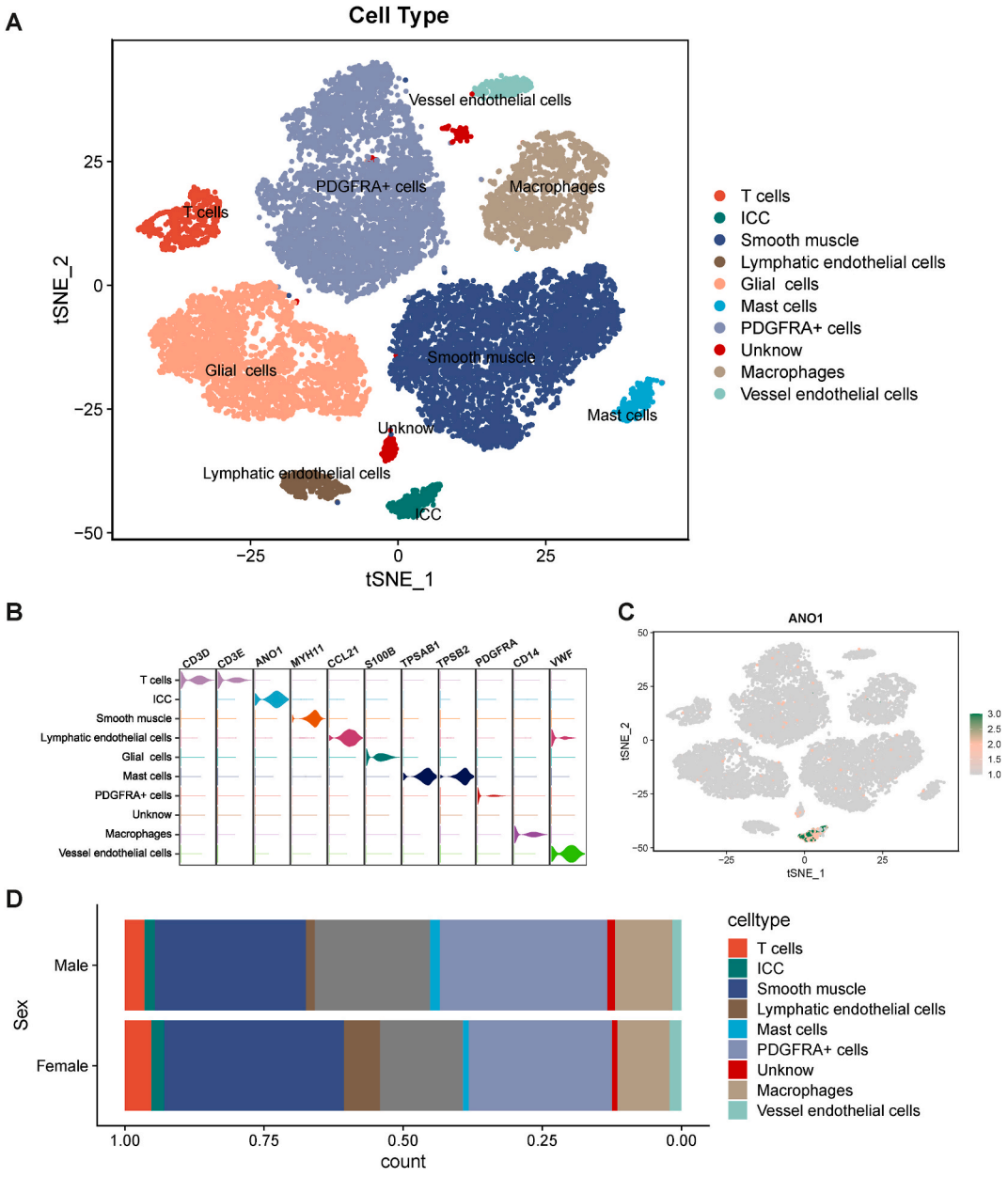

Fig. 3. Cell type constitution of the colon tissues. (A) t-SNE plots of cells from fourteen patients (14 samples). Colors represent cell types. Cells were clustered into 10 sub-clusters based on biological annotation. Each dot represents a single cell. (B) Violin plot of proportion of cells in the respective cluster expressing selected marker genes. Violin size represents the percentage of cells that express the gene. (C) Expression of the ANO1 at the single cell level. (D) The proportion of different cell types in sex.

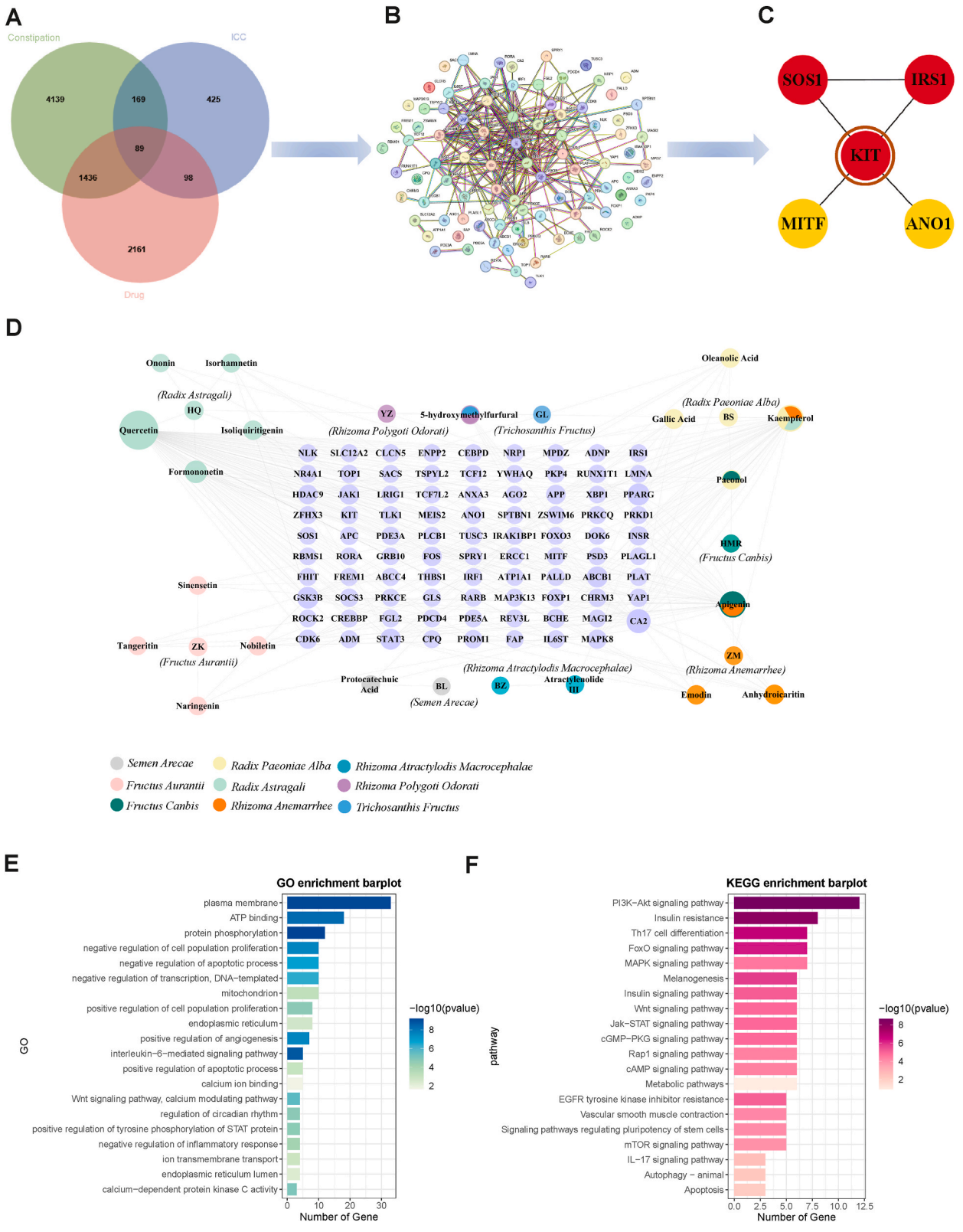

Fig. 4. KIT is a core target for QLF targeting ICC against constipation. (A) Venn diagram of overlapping of ICC related constipation targets and QLF targets. (B) Establishment of PPI network of the QLF targeting ICC against constipation targets using STRING database (version 12.0). (C) Five hub targets. (D) Drug-ingredient-target network. (E) The top 20 significantly enriched GO and (F) KEGG pathways for the 89 QLF targets.

3.2. QLF showed great efficacy in the treatment of constipation

3.2.1. QLF promoted the laxative effect in constipated rats

Measurement of rat body weight, fecal number at 4 h and 24 h, first stool passed time, fecal moisture content and intestinal propulsion rate were conducted to evaluate their defecation function. As shown in Fig. 2A, there were no significant differences in body weight among the experimental groups of rats. Compared to the NC group, the defecation function of the MC group was noticeably impaired. Two weeks after treatment with QLF, fecal number significantly increased in the various concentration gradient QLF groups and the PC group ($p < 0.001$). Additionally, the first stool passed time was significantly shortened in the HQLF group ($p < 0.01$) and fecal moisture content significantly increased in the MQLF and HQLF groups ($p < 0.001$). Similarly, the MQLF, HQLF, and PC groups exhibited a similar increasing trend in intestinal propulsion rate ($p < 0.001$). QLF can significantly improve the defecation function of constipated rats induced by compound diphenoxylate.

3.2.2. QLF regulated intestinal neurotransmitters in serum of constipated rats

Neurotransmitters are closely related to intestinal motility [22]. The serum levels of AChE, MTL, SP, GAS, VIP and 5-HT were measured respectively. As shown in Fig. 2B, AChE level was significantly reduced in MC group compared with NC group, while QLF treatment could improve AChE level, especially in HQLF group. 5-HT levels showed a similar trend to AChE levels in all experimental groups. However, VIP levels increased significantly in MC group compared to NC group and after treatment, HQLF levels approached those in NC group. In addition, MTL, SP and GAS levels increased significantly in both QLF and PC group.

3.2.3. QLF protected the intestines from injury in constipated rats

HE staining showed that there were no pathological changes in NC group. In MC group, the mucus layer was thinned, goblet cells were reduced, and inflammatory cell infiltration was seen in some epithelium. Compared to those in MC group,the number of goblet cells in PC, MQLF and HQLF groups improved, the glands arranged more neatly, inflammatory cells decreased, and the mucus layer thickened sequentially significantly, especially in the HQLF group.In general, QLF could restore the pathological and morphological damage of intestinal tissue in rats with constipation induced by compound diphenoxylate(Fig. 2C).

After compound diphenoxylate induction, the ICC in the MC group showed mitochondrial swelling and autophagy and part of the rough endoplasmic reticulum expanded obviously. After treatment with QLF, ICC recovered some structural integrity but most mitochondria in the cytoplasm had mild swelling and a small number of autophagosomes could be seen. After treatment with mosapride citrate, compared with MQLF group, the structure was abnormal, mitochondria swelled significantly, crists were broken, dissolved or even disappeared, rough endoplasmic reticulum expanded to different degrees to form vesicles, and ribosomes on the surface of endoplasmic reticulum fell off and depolymerized (Fig. 2D).

3.2.4. QLF upregulated 5-HT4R and CX43 protein expression

Due to the significant roles of 5-HT and CX43 in the treatment of constipation, we further examined the protein expression of 5-HT4R and CX43. The results revealed a marked decrease in the protein expression of 5-HT4R and CX43 in the MC group. However, following QLF treatment, there was a significant increase in the protein expression levels of 5-HT4R and CX43. The trend of mRNA expression was consistent with that of protein expression ($p < 0.05$) (Fig. 2E).

3.3. Network pharmacology analysis

3.3.1. Identification of ICC-related targets

We followed the previously described procedure, including quality control, normalization, batch effect removal, and calibration. We successfully identified 19,068 cells and classified them into 18 distinct cell clusters. After manual merging and annotation, we ultimately presented 10 unique cell clusters (Fig. 3A) [23,24]. Then, we annotated the clusters based on several canonical marker genes for known cell lineages: T cell (CD3D, CD3E), ICC (ANO1), smooth muscle (MYH11), lymphatic endothelial cell (CCL21), glial cell (S100B), $PDGFRA^{+}$ cell (PDGFRA), macrophages (CD14), mast cell (TPSAB1, TPSB2), Vessel endothelial cell (VWF) and unknow (Fig. 3B). To obtain an overview of the distribution of ICC, we generated a t-SNE plot to visualize its distribution (Fig. 3C). Subsequently, we created a bar chart based on patient gender to display the proportions of the 10 cell types categorized by their labels (Fig. 3D). In the end, 781 ICC-related targets were identified.

3.3.2. Construction of the networks

A total of 3784 QLF drug targets were obtained after removing duplicates through Herb, ITCM database and manual retrieval. 781 ICC-related targets were screened from scRNA-seq data and 5833 targets were associated with constipation in Genecards database. After taking the intersection of the two, 258 ICC-related targets were obtained.

The drug targets were combined with the ICC-related constipation targets, resulting in a total of 89 targets for QLF targeting ICC against constipation (Fig. 4A). To construct the PPI network, 89 therapeutic targets were uploaded to the STRING. The PPI network consists of 74 nodes and 452 edges, with an average node degree of 12.22 (Fig. 4B). Then KIT, SOS1, IRS1, ANO1 and MITF were selected as hub targets according to cytoHubba plug-ins (Fig. 4C).

Cytoscape software was utilized to further construct the herb-ingredient-target network of QLF active ingredients and potential therapeutic targets relevant for constipation treatment. Collectively, 7 ingredients attributed to Radix Astragali, 4 attributed to Fructus Aurantii, 4 attributed to Radix Paeoniae Alba, 3 attributed to Rhizoma Anemarrhee, 2 attributed to Fructus Canbis, 1 attributed to

Rhizoma Atractylodis Macrocephalae, 1 attributed to Semen Arecae, 1 attributed to Rhizoma Polygoti Odorati and Trichosanthis Fructus (Fig. 4D).

3.3.3. GO and KEGG enrichment analysis

GO and KEGG enrichment analysis of targets for QLF targeting ICC against constipation were performed in KOBAS database. As shown in Fig. 4D, the targets mainly regulate plasma membrane, calcium ion binding, calcium-dependent protein kinase C activity,

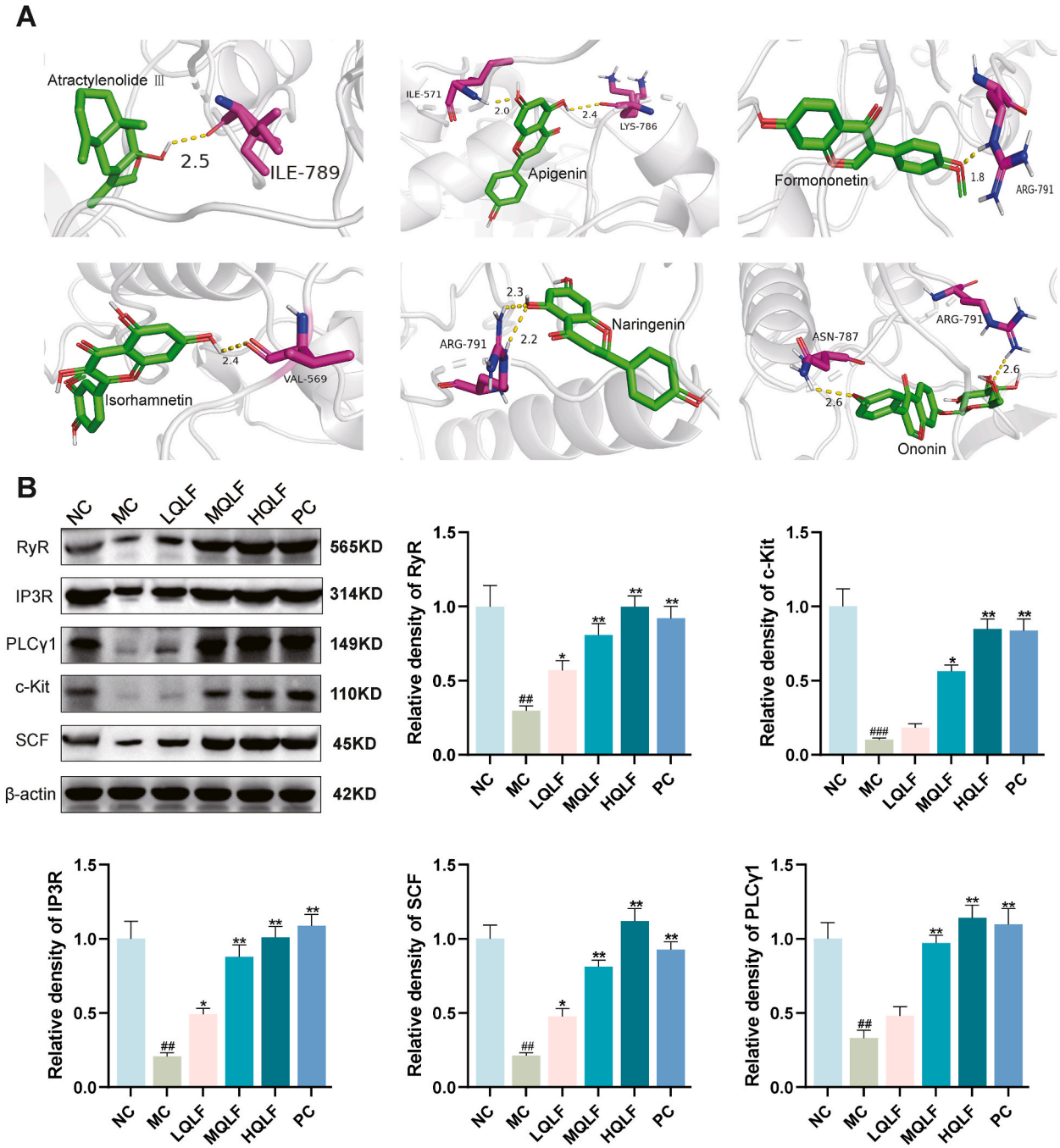

Fig. 5. QLF could upregulate the SCF/c-kit signaling pathway. (A) Pattern diagram of molecular docking of Atractylenolide III, Apigenin, Formononetin, Isorhamnetin, Naringenin, and Ononin with KIT (PDB ID: 6MOB). (B) The protein levels of SCF/c-kit signaling pathway in colon tissue detected by Western blotting assay, n = 6. Data are expressed as mean ± SD. $^{\#}p < 0.05$, $^{\#\#}p < 0.01$, $^{\#\#\#}p < 0.001$, compared to the NC group. $^{*}p < 0.05$, $^{**}p < 0.01$, $^{***}p < 0.001$, compared to the MC group.

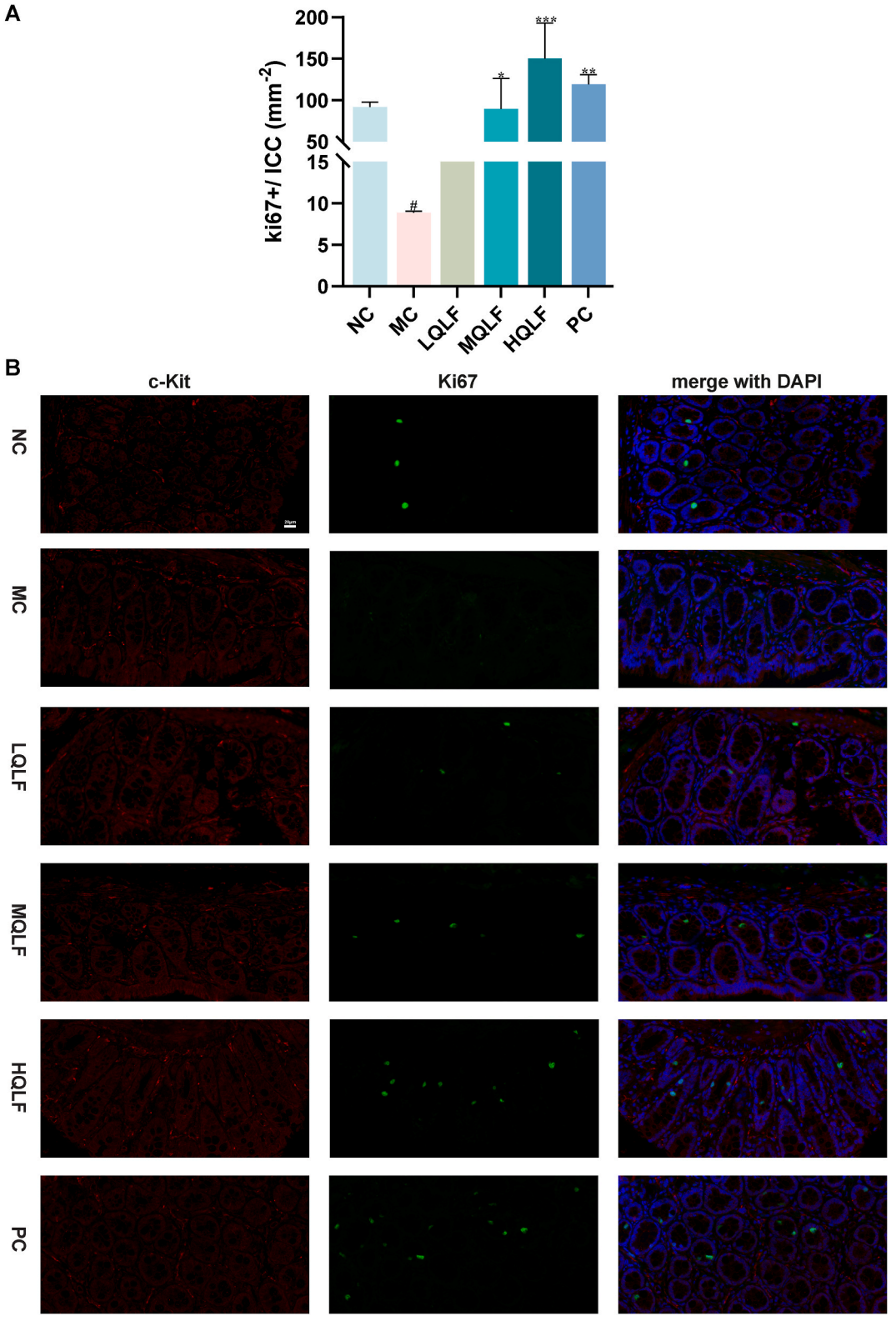

Fig. 6. QLF could promote ICC proliferation. (A) The proliferation of intestinal cajal cells in each group was detected by Ki67 and c-kit double standard immunofluorescence staining, n = 3. Data are expressed as mean ± SD. $^{\#}p < 0.05$, compared to the NC group. $^{*}p < 0.05$, $^{**}p < 0.01$, $^{***}p < 0.001$, compared to the MC group. (B) Representative images showing the localization of ki67 (green), c-Kit (red) and the nucleus (DAPI, blue).

positive regulation of cell population proliferation and negative regulation of apoptotic process. As shown in Fig. 4F, based on the ascending order of P-values, KEGG enrichment analysis is primarily associated with PI3K-Akt signaling, Wnt signaling pathway, MAPK signaling pathway, Jak-STAT signaling pathway, and mTOR signaling pathway.

3.4. Molecular docking

Molecular docking studies indicate that key ingredients of QLF were well combined with KIT. The outcomes of the molecular docking procedure were depicted in Supplementary Fig. S2. The findings indicated that KIT exhibited the most robust and enduring binding affinity with Atractylenolide III and Apigenin (−7.9 kcal/mol), followed by Formononetin, Isorhamnetin, Naringenin and Ononin (−7.8 kcal/mol) (Fig. 5A).

3.5. QLF stimulated the SCF/c-kit signaling pathway

The previous research has identified c-Kit as a key target for QLF in treating ICC-related constipation. (Fig. 4C). As widely known, c-Kit is considered a marker gene for ICC. The SCF/c-Kit and its downstream signaling pathway are closely associated with phenotypic changes in ICC. Among these downstream components, the PLCγ1-IP3 signaling axis plays a role in various cellular functions such as motility and proliferation. We hypothesize that QLF may restore ICC function by upregulating the SCF/c-Kit pathway and its downstream signaling. The Western blot results confirm that, compared to the MC group, after QLF treatment, the expression levels of proteins related to the SCF/c-Kit signaling pathway, including SCF, c-Kit, PLCγ1, IP3R, and RyR, were increased. The trend of mRNA expression was consistent with that of protein expression ($p < 0.05$) (Fig. 5B).

3.6. QLF promoted ICC proliferation

In order to elucidate how QLF affects the phenotype of ICC, we employed anti-Ki67 antibodies to assess the presence of proliferative ICC. The results indicated that in the MC group, there were few c-Kit+/Ki67+ double-labeled cells. In contrast, the QLF treatment group exhibited a higher density of c-Kit+/Ki67+double-labeled cells (Fig. 6).

4. Discussion

Constipation not only takes a toll on a patient's physical and mental well-being but also places a significant financial strain on the healthcare system. Traditional Chinese Medicine approaches disease treatment with a multi-faceted strategy, encompassing various ingredients, targets, pathways, and mechanisms [8]. It is known for its minimal side effects, reduced chances of recurrence, and pronounced effectiveness. QLF has achieved good clinical results in the treatment of constipation. In a randomized controlled trial, the overall clinical effectiveness rate of QLF for constipation was as high as 91.1% [25]. In addition, several herbs of QLF, such as *Fructus Aurantii, Radix Astragali*, and *Rhizoma Atractylodis*, have been used for centuries in the treatment of constipation [26]. However, the mechanism of QLF in treating constipation is still largely unknown. In this study, we discovered that, in rats with constipation, QLF significantly improved intestinal motility, increased the moisture content of feces, modulated intestinal neurotransmission, and up-regulated the SCF/c-Kit pathway to restore the ICC phenotype.

Traditional techniques can only identify a few highly active ingredients in herbal formulations, failing to systematically depict the complex efficacy network of traditional medicine. Single-cell omics technology could enhance the study of the targets of traditional Chinese medicine, providing more precise experimental data and further constructing a "drug-ingredient-cell target" spatial regulation network. An increasing number of traditional Chinese medicine studies are utilizing single-cell technology to explore the microscopic effects of herbal formulations on cells [27,28]. We searched the GEO database for suitable single-cell data and combined it with network pharmacology, identifying the targets of QLF in treating constipation by targeting ICCs, and conducted subsequent research on the core targets.

Rhythmic slow waves of gastrointestinal muscle contraction are mediated by a variety of cell types, including smooth muscle cells, enteric neurons, telocytes, and ICC [29]. ICC mediates nerve and smooth muscle cells and regulates the transmission of neuromuscular signals, thereby controlling the contraction and peristalsis of the corresponding digestive tract smooth muscle [30]. Abnormalities in the number and structure of ICCs are associated with some gastrointestinal motility disorders [29], such as functional dyspepsia (FD) [31], intestinal obstruction [32], Hirschsprung disease (HSCR) and constipation [33,34]. The SCF/c-Kit signaling pathway is crucial for the normal development, maturation, and survival of ICCs. It is essential for maintaining the phenotype and function of the ICC network [35], therefore, KIT is widely used to specifically detect ICCs.

Gastrointestinal motility is regulated by gastrointestinal hormones, 5-HT is an important neurotransmitter in the enteric nervous system, and about 95% of 5-HT is produced in the gastrointestinal tract, which contributes to electrolyte secretion and absorption and intestinal peristalsis [36]. 5-HT4R is an important 5-HT excitatory receptor that is widely present in the gastrointestinal tract. 5-HT4R is a structurally active Gs-coupled 5-HT receptor, and the distribution of 5-HT4R in intestinal smooth muscle can directly regulate the movement of smooth muscle [37], playing a central role in gastrointestinal motility. In the intermuscular plexus, 5-HT4R promotes the release of neurotransmitters from the cholinergic system, thereby improving gastrointestinal smooth muscle contraction. In addition, 5-HT4R can increase secretion-enhancing pacing of ICCs [38]. Endocrine disorders and neurologic deficits may lead to abnormal and inactivation of gastrointestinal hormone secretion, leading to further gastrointestinal dysfunction. Therefore, changing hormone levels will promote gastrointestinal motility. Our study found that QLF treatment not only reversed the recovery of neurotransmitters such as

motilin, substance P, somatostatin, endothelin, and vasoactive intestinal peptide, but also upregulated the expression of c-Kit and SCF. In addition, the number of goblet cells and mucus layer thickness increased after QLF treatment, suggesting that improving gastrointestinal hormone secretion may be one of the key mechanisms of QLF in intestinal motility. Recent studies have revealed that a class of connexins found in colonic epithelial cells is strongly associated with gastrointestinal slow waves and gastrointestinal dyskinesia, and the expression of CX43 protein in the intestinal mucosa of patients with functional constipation is significantly reduced. ICCs are connected to other ICCs and smooth muscle cells through gap junction to form syncytia in gastrointestinal tissues [11], CX43 is the main connexin of human slit junction, and its expression change is closely related to the occurrence of gastrointestinal diseases such as gastrointestinal tumors, Hirschsprung disease, and functional dyspepsia. Decreased expression of CX43 might lead to weakened cell-to-cell communication, suggesting that the onset of constipation may be related to the destruction of the gap junction between cells. The expression of CX43 in the model group we studied was reduced, so it can be seen that CX43 as a channel changes, so that the electrophysiological signals of the colon cannot be produced, and also affect the signal transmission to the smooth muscle of the colon, which in turn leads to colonic motility disorders, which may be one of the important mechanisms causing constipation [39].

In this study, we observed that QLF elevated the protein levels of c-Kit, SCF, PLCγ1, RyR, and IP3R in rat colon tissue. This suggested that QLF might enhance intestinal motility by promoting the expression of SCF/c-Kit and its downstream pathway proteins, thereby reversing the phenotype of ICC. To comprehensively understand the effects of QLF on the SCF/c-Kit signaling pathway, we employed immunofluorescence to assess the proliferation of ICCs in different groups. Our results indicated that there was no significant ICC proliferation in the rats from the model group, but QLF seemed to augment ICC proliferation. c-Kit activation is followed by the recruitment and activation of several downstream signaling molecules including Erk 1/2, Grb2, p38 MAPK, SFK and PLCγ [40–42]. There was a relationship between PLCγ activity and autophagy for the two hydrolysis products of PIP2 induced by PLC (IP3 and DAG). IP3 could activate IP3R to bidirectionally regulate autophagy [43]. IP3R can also be combined with Beclin1 (IP3 bound domain via IP3R) and Bcl-2 (transduction domain in the middle of regulation and IP3R) to form Beclin1-IP3R-Bcl-2 complexes. This study indicated that the ICCs in the model group showed morphological mitochondrial swelling and autophagy, with a noticeable enlargement of some parts of the rough endoplasmic reticulum. This suggested that ICCs in constipated rats might have experienced excessive autophagy. However, after QLF intervention, the ICCs regained structural integrity to some extent, suggesting that QLF might inhibit excessive autophagy in ICCs of constipated rats.

However, there are some limitations to this study. First, we only verified the preliminary mechanism through molecular docking and in vivo experiments, not in vitro experiments. Secondly, we did not set up a target inhibitor group or agonist group for response experiments. Thirdly, single cell transcriptome sequencing was not performed on colon tissues of constipated rats before and after drug treatment. Therefore, further in vitro and in vivo experiments as well as multi-omics experimental methods are needed to confirm the mechanism and effect of QLF against constipation by targeting ICC, so as to provide scientific basis for clinical application.

5. Conclusion

In summary, our research findings confirmed the laxative effect of QLF on constipated rats. Furthermore, this study represented the first exploration of its underlying mechanisms. The results indicated that QLF improved intestinal motility by modulating neurotransmitters and restoring intercellular gap junctions within the colon. Additionally, QLF may also have enhanced intestinal peristalsis by activating the SCF/c-Kit-PLCγ1-IP3R/RYR axis, thereby promoting the proliferation of ICCs and enhancing intestinal motility. Collectively, we reported that QLF was a traditional Chinese medicine that targeted ICCs to regulate intestinal motility disorders, promoted ICC proliferation in constipated rats. These findings broadened our understanding of c-Kit as a target protein for ICC repair and opened up new avenues for innovative treatments for constipation-related injuries. Moreover, this study revealed the direct pharmacological targets of QLF from the perspective of ICC repair, providing a scientific basis for the clinical application of QLF.

Ethics and consent statement

This study was reviewed and approved by Committee of Shanghai Traditional Chinese Medicine Hospital with the approval number: NO.202201, dated February 9, 2022.

Data availability statement

All data are fully available without restriction.

CRediT authorship contribution statement

Jiacheng Li: Writing – review & editing, Writing – original draft, Software, Methodology, Data curation, Conceptualization. **Yugang Fu:** Writing – review & editing, Data curation. **Yanping Wang:** Visualization, Investigation. **Yiyuan Zheng:** Validation, Software. **Kehui Zhang:** Validation, Software. **Yong Li:** Writing – review & editing, Supervision, Funding acquisition.

Declaration of competing interest

The authors declare that they have no known competing financial interests or personal relationships that could have appeared to influence the work reported in this paper.

Acknowledgements

This research was supported by Shanghai Science and Technology Innovation Action Plan Biomedical Technology Support Project (22S21901100) and Future Plan for Traditional Chinese Medicine development of Science and Technology of Shanghai Municipal Hospital of Traditional Chinese Medicine (WL-YBXM-2022002K).

Appendix A. Supplementary data

Supplementary data to this article can be found online at https://doi.org/10.1016/j.heliyon.2024.e31860.

References

[1] B. Barberio, C. Judge, E.V. Savarino, A.C. Ford, Global prevalence of functional constipation according to the Rome criteria: a systematic review and meta-analysis, Lancet Gastroenterol Hepatol 6 (8) (2021) 638–648.
[2] S.S. Rao, K. Rattanakovit, T. Patcharatrakul, Diagnosis and management of chronic constipation in adults, Nat. Rev. Gastroenterol. Hepatol. 13 (5) (2016) 295–305.
[3] I.M. Paquette, M. Varma, C. Ternent, G. Melton-Meaux, J.F. Rafferty, D. Feingold, et al., The American society of colon and rectal surgeons' clinical practice guideline for the evaluation and management of constipation, Dis. Colon Rectum 59 (6) (2016) 479–492.
[4] G. Lindberg, S.S. Hamid, P. Malfertheiner, O.O. Thomsen, L.B. Fernandez, J. Garisch, et al., World Gastroenterology Organisation global guideline: constipation–a global perspective, J. Clin. Gastroenterol. 45 (6) (2011) 483–487.
[5] F.M. Schmidt, V.L. Santos, Prevalence of constipation in the general adult population: an integrative review, J. Wound, Ostomy Cont. Nurs. 41 (1) (2014) 70–76.
[6] Z. Chen, Y. Peng, Q. Shi, Y. Chen, L. Cao, J. Jia, et al., Prevalence and risk factors of functional constipation according to the Rome criteria in China: a systematic review and meta-analysis, Front. Med. 9 (2022) 815156.
[7] E.P. Cherniack, Use of complementary and alternative medicine to treat constipation in the elderly, Geriatr. Gerontol. Int. 13 (3) (2013) 533–538.
[8] L. Wang, F. Wu, Y. Hong, L. Shen, L. Zhao, X. Lin, Research progress in the treatment of slow transit constipation by traditional Chinese medicine, J. Ethnopharmacol. 290 (2022) 115075.
[9] X. Zhao, Y. Fang, J. Ye, F. Qin, W. Lu, H. Gong, A meta-analysis of randomized controlled trials of a traditional Chinese medicine prescription, modified RunChang-Tang, in treating functional constipation, Medicine (Baltim.) 100 (20) (2021) 25760.
[10] X. Zhou, H. Qian, D. Zhang, L. Zeng, Inhibition of autophagy of Cajal mesenchymal cells by gavage of tong bian decoction based on the rat model of chronic transit constipation, Saudi J. Biol. Sci. 27 (2) (2020) 623–628.
[11] T. Komuro, Structure and organization of interstitial cells of Cajal in the gastrointestinal tract, J Physiol 576 (3) (2006) 653–658.
[12] P.J. Blair, P.L. Rhee, K.M. Sanders, S.M. Ward, The significance of interstitial cells in neurogastroenterology, J Neurogastroenterol Motil 20 (3) (2014) 294–317.
[13] K.M. Sanders, S.M. Ward, S.D. Koh, Interstitial cells: regulators of smooth muscle function, Physiol. Rev. 94 (3) (2014) 859–907.
[14] G. Farrugia, Interstitial cells of Cajal in health and disease, Neuro Gastroenterol. Motil. 20 (2008) 54–63.
[15] C.J. Streutker, J.D. Huizinga, D.K. Driman, R.H. Riddell, Interstitial cells of Cajal in health and disease. Part I: normal ICC structure and function with associated motility disorders, Histopathology 50 (2) (2007) 176–189.
[16] J.D. Huizinga, L. Thuneberg, M. Klüppel, J. Malysz, H.B. Mikkelsen, A. Bernstein, W/kit gene required for interstitial cells of Cajal and for intestinal pacemaker activity, Nature 373 (6512) (1995) 347–349.
[17] S.J. Hwang, P.J. Blair, F.C. Britton, K.E. O'Driscoll, G. Hennig, Y.R. Bayguinov, et al., Expression of anoctamin 1/TMEM16A by interstitial cells of Cajal is fundamental for slow wave activity in gastrointestinal muscles, J Physiol 587 (20) (2009) 4887–4904.
[18] M.H. Zhu, T.W. Kim, S. Ro, W. Yan, S.M. Ward, S.D. Koh, et al., A Ca(2+)-activated Cl(-) conductance in interstitial cells of Cajal linked to slow wave currents and pacemaker activity, J Physiol 587 (20) (2009) 4905–4918.
[19] T. Wedel, J. Spiegler, S. Soellner, U.J. Roblick, T.H. Schiedeck, H.P. Bruch, et al., Enteric nerves and interstitial cells of Cajal are altered in patients with slow-transit constipation and megacolon, Gastroenterology 123 (5) (2002) 1459–1467.
[20] H. Yang, H. Luo, Y.H. Li, Effects of epidural infusion of morphine combined with small-dose naloxone on gastrointestinal interstitial cells of Cajal in rabbits, Eur. Rev. Med. Pharmacol. Sci. 23 (6) (2019) 2596–2601.
[21] S. Schneider, S.K. Hashmi, A.J. Thrasher, D.R. Kothakapa, C.M. Wright, R.O. Heuckeroth, Single nucleus sequencing of human colon myenteric plexus-associated visceral smooth muscle cells, platelet derived growth factor receptor alpha cells, and interstitial cells of cajal, Gastro Hep Adv 2 (3) (2023) 380–394.
[22] X. Zhou, B. Mao, X. Tang, Q. Zhang, J. Zhao, H. Zhang, et al., Exploring the dose-effect relationship of bifidobacterium longum in relieving loperamide hydrochloride-induced constipation in rats through colon-released capsules, Int. J. Mol. Sci. 24 (7) (2023) 6585.
[23] J. Li, Y. Fu, K. Zhang, Y. Li, Integration of bulk and single-cell RNA-seq data to construct a prognostic model of membrane tension-related genes for colon cancer, Vaccines (Basel) 10 (9) (2022) 1562.
[24] X. Cheng, Y. Wei, Y. Fu, J. Li, L. Han, A novel enterocyte-related 4-gene signature for predicting prognosis in colon adenocarcinoma, Front. Immunol. 13 (2022) 1052182.
[25] M. Zhou, Y. Chen, L. Lin, X. Guo, Y. Li, Effect of Jiawei Qi-Lang Decoction on fecal short-chain fatty acides in patients with drug dependent constipation, Chin. J. Microecol. 34 (9) (2022) 1061–1065.
[26] X.M. Wang, L.X. Lv, Y.S. Qin, Y.Z. Zhang, N. Yang, S. Wu, et al., Ji-Chuan decoction ameliorates slow transit constipation via regulation of intestinal glial cell apoptosis, World J. Gastroenterol. 28 (34) (2022) 5007–5022.
[27] K. Jin, S. Gao, P. Yang, R. Guo, D. Li, Y. Zhang, et al., Single-cell RNA sequencing reveals the temporal diversity and dynamics of cardiac immunity after myocardial infarction, Small Methods 6 (3) (2022) 2100752.
[28] G. Deng, L. Zhou, B. Wang, X. Sun, Q. Zhang, H. Chen, et al., Targeting cathepsin B by cycloastragenol enhances antitumor immunity of CD8 T cells via inhibiting MHC-I degradation, J Immunother Cancer 10 (10) (2022) 4874.
[29] D. Foong, J. Zhou, A. Zarrouk, V. Ho, M.D. O'Connor, Understanding the biology of human interstitial cells of cajal in gastrointestinal motility, Int. J. Mol. Sci. 21 (12) (2020) 4540.
[30] Y. Wang, H. Jiang, L. Wang, H. Gan, X. Xiao, L. Huang, et al., Arctiin alleviates functional constipation by enhancing intestinal motility in mice, Exp. Ther. Med. 25 (5) (2023) 199.
[31] L. Li, Q. Jia, X. Wang, Y. Wang, C. Wu, J. Cong, et al., Chaihu Shugan San promotes gastric motility in rats with functional dyspepsia by regulating Drp-1-mediated ICC mitophagy, Pharm. Biol. 61 (1) (2023) 249–258.
[32] L. Li, C. Zou, Z. Zhou, X. Wang, X. Yu, Phenotypic changes of interstitial cells of Cajal after intestinal obstruction in rat model, Braz. J. Med. Biol. Res. 52 (10) (2019) 8343.
[33] A. Gu, Z. Wu, P. Wang, J. Liu, J. Wang, Q. Wang, et al., Downregulation of ICCs and PDGFRα+ cells on colonic dysmotility in hirschsprung disease, Front Pediatr 10 (2) (2022) 975799.

[34] G.L. Lyford, C.L. He, E. Soffer, T.L. Hull, S.A. Strong, A.J. Senagore, et al., Pan-colonic decrease in interstitial cells of Cajal in patients with slow transit constipation, Gut 51 (4) (2002) 496–501.
[35] Y.Y. Tan, Z.L. Ji, G. Zhao, J.R. Jiang, D. Wang, J.M. Wang, Decreased SCF/c-kit signaling pathway contributes to loss of interstitial cells of Cajal in gallstone disease, Int. J. Clin. Exp. Med. 7 (11) (2014) 4099–4106.
[36] Y. Zhan, Y. Wen, L.J. Du, X.X. Wang, S.Y. Tang, P.F. Kong, et al., Effects of maren pills on the intestinal microflora and short-chain fatty acid profile in drug-induced slow transit constipation model rats, Front. Pharmacol. 13 (2022) 804723.
[37] R. Wang, X. Lu, L. Zhao, W. Zhang, S. Zhang, Houpo paiqi mixture promotes intestinal motility in constipated rats by modulating gut microbiota and activating 5-HT-cAMP-PKA signal pathway, J. Appl. Microbiol. 134 (8) (2023) 153.
[38] Y. Zhu, J. Cheng, J. Yin, Y. Yang, J. Guo, W. Zhang, et al., Effects of sacral nerve electrical stimulation on 5-HT and 5-HT3AR/5-HT4R levels in the colon and sacral cord of acute spinal cord injury rat models, Mol. Med. Rep. 22 (2) (2020) 763–773.
[39] X. Liang, D. Wan, Y. Cai, W. Yue, X. Wang, H. Zhou, et al., Xuanhuang runtong tablets relieve slow transit constipation in mice by regulating TLR5/IL-17a signaling mediated by gut microbes, Evid Based Complement Alternat Med 2023 (2023) 6506244.
[40] K. Thömmes, J. Lennartsson, M. Carlberg, L. Rönnstrand, Identification of Tyr-703 and Tyr-936 as the primary association sites for Grb2 and Grb7 in the c-Kit/stem cell factor receptor, Biochem. J. 341 (1) (1999) 211–216.
[41] J. Lennartsson, C. Wernstedt, U. Engström, U. Hellman, L. Rönnstrand, Identification of Tyr900 in the kinase domain of c-Kit as a Src-dependent phosphorylation site mediating interaction with c-Crk, Exp. Cell Res. 288 (1) (2003) 110–118.
[42] J.L. Gommerman, D. Sittaro, N.Z. Klebasz, D.A. Williams, S.A. Berger, Differential stimulation of c-Kit mutants by membrane-bound and soluble Steel Factor correlates with leukemic potential, Blood 96 (12) (2000) 3734–3742.
[43] L. Dai, X. Chen, X. Lu, F. Wang, Y. Zhan, G. Song, et al., Phosphoinositide-specific phospholipase Cγ1 inhibition induces autophagy in human colon cancer and hepatocellular carcinoma cells, Sci. Rep. 7 (1) (2017) 13912.